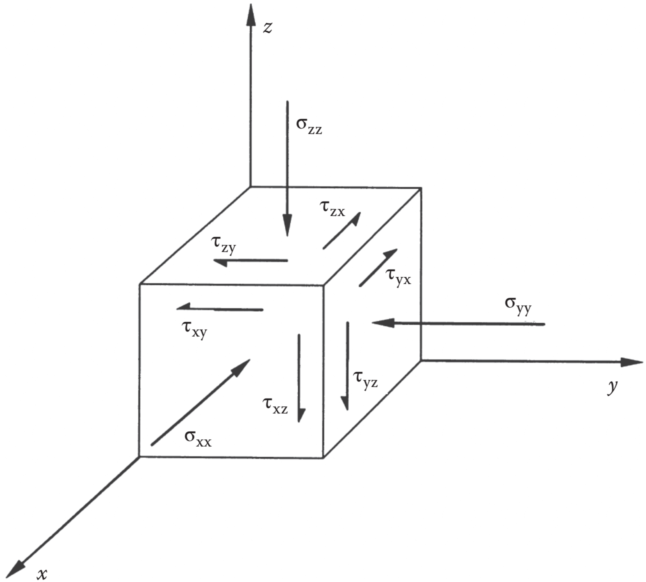

Figure 2.1 General three-dimensional state of stress. The faces of the cubic element shown are termed the *positive faces*, because the outward normals are in the positive directions of x, y and z. On the faces not shown (the *negative faces*), the directions of the stresses are reversed in order to satisfy to condition of equilibrium.

002x001.eps

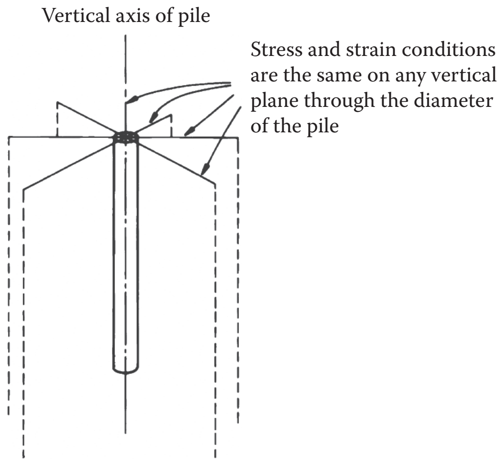

Figure 2.2 Axisymmetry.

002x002.eps

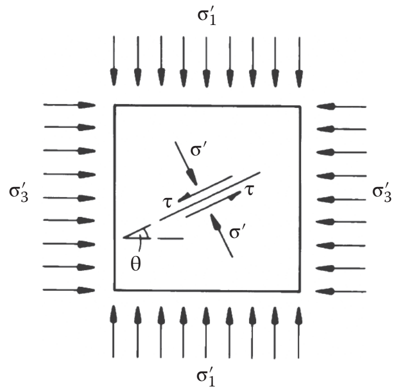

Figure 2.3 Normal and shear stresses acting on an imaginary cut within the cross-sectional plane of a long geotechnical construction.

002x003.eps

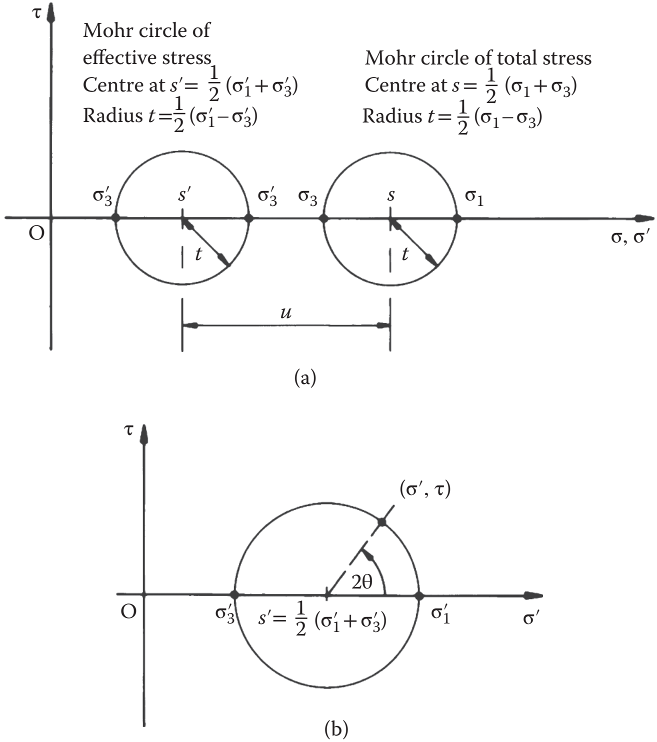

Figure 2.4 Mohr circles of stress showing (a) the circles representing total and effective stress separated by the pore water pressure, u; and (b) the stress state on an imaginary 'cut' at an angle θ anticlockwise from the plane on which the major principal effective stress acts.

002x004.eps

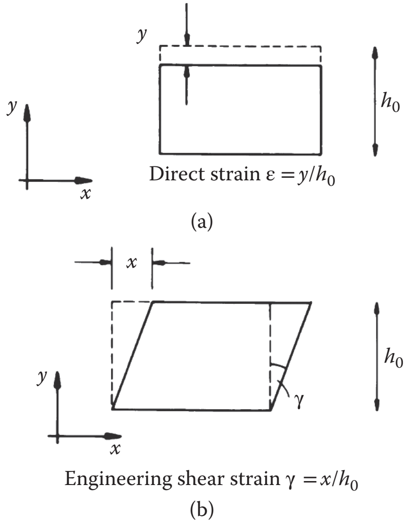

Figure 2.5 Strain: (a) direct strain and (b) engineering shear strain.

002x005.eps

Courtesy of CRC Press/Taylor & Francis Group

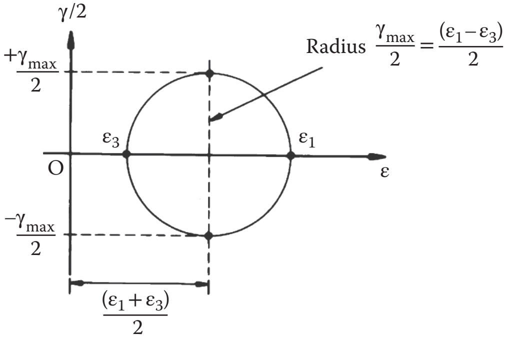

Figure 2.6 Mohr circle of strain.

002x006.eps

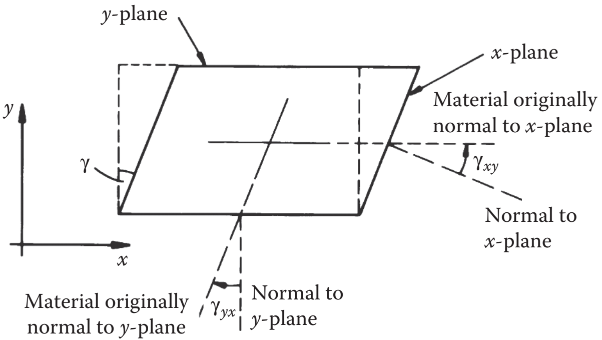

Figure 2.7 True shear strain.

002x007.eps

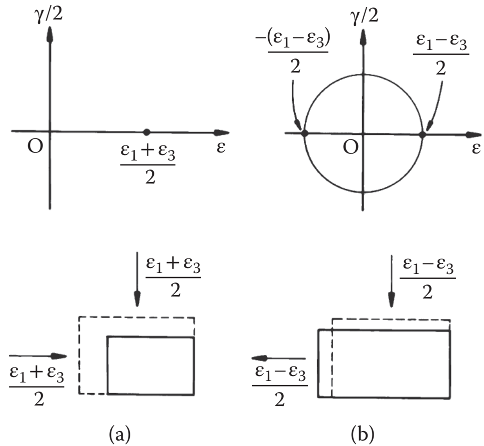

Figure 2.8 (a) Uniform compression. (b) Pure shear.

002x008.eps

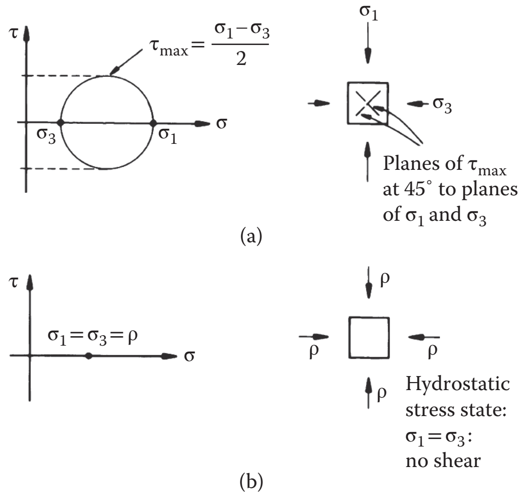

Figure 2.9 Mohr circles of stress for the plane containing the major and minor principal stresses. (a) Material which is able to resist shear stress. (b) Material which is unable to resist shear stress.

002x009.eps

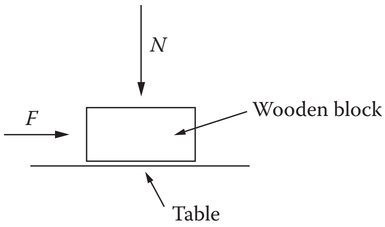

Figure 2.10 Wooden block on a wooden table.

002x010.eps

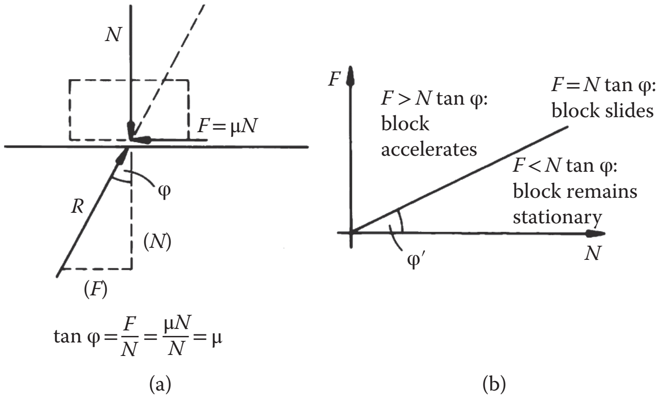

Figure 2.11 (a) Angle of inclination of resultant force on the interface; (b) relationship between F and N when the block starts to slide.

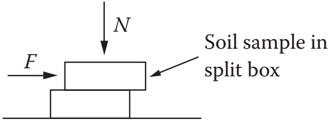

Figure 2.12 Sliding interface (shearbox) test to investigate frictional characteristics of a soil.

002x012.eps

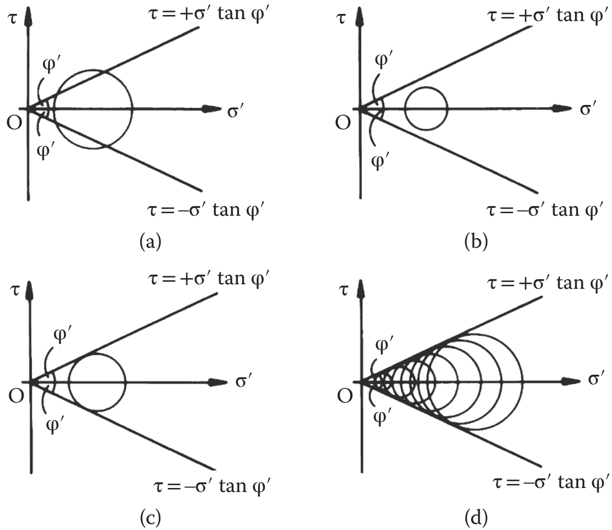

Figure 2.13 Combinations of shear stress and normal effective stress: (a) impossible stress state, (b) permissible stress state with soil not at failure, and (c) permissible stress state with soil on verge of failure (limiting stress state). (d) The lines $\tau = \pm\sigma \tan \varphi$ as an envelope to all possible limiting stress states.

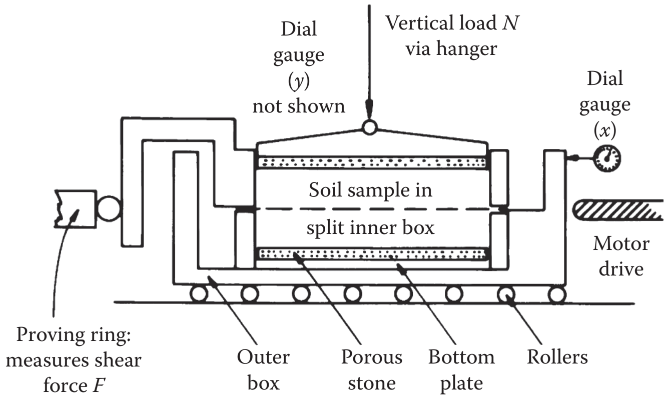

Figure 2.14 Standard shearbox apparatus.

002x014.eps

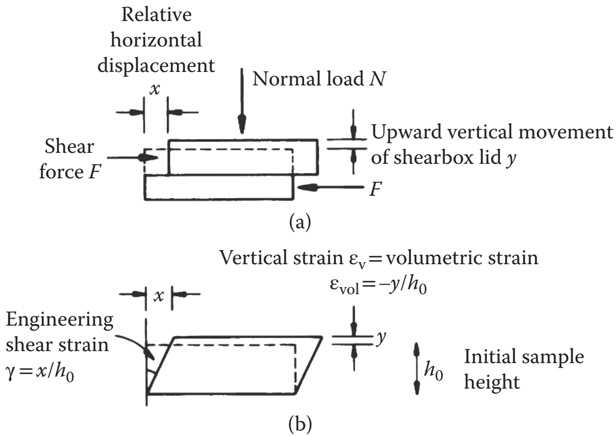

Figure 2.15 Schematic deformation of shearbox sample, showing quantities measured during shear test: (a) actual deformation and (b) idealised deformation.

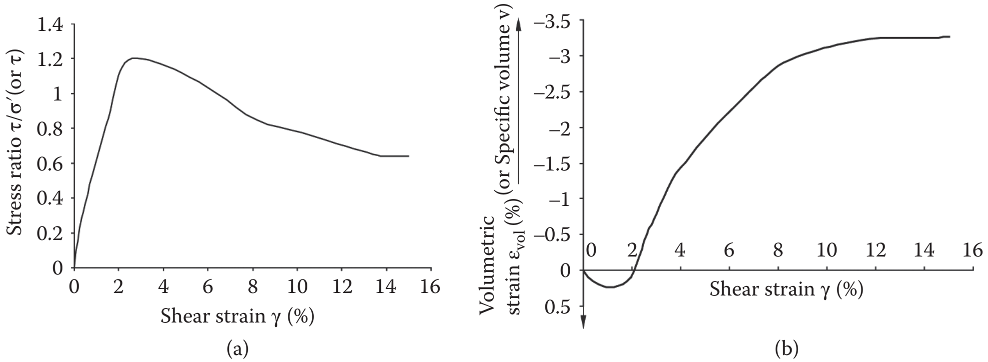

Figure 2.16 Shearbox test data plotted as: (a) τ/σ' (or τ) vs γ, and (b) ε_{vol} (or ν) vs γ.

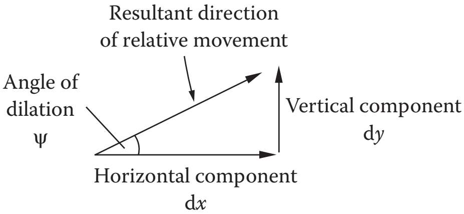

Figure 2.17 Dilation.

002x017.eps

(a) (b)

Figure 2.18 Conceptual model for: (a) compression and (b) dilation during shear.

002x018.eps

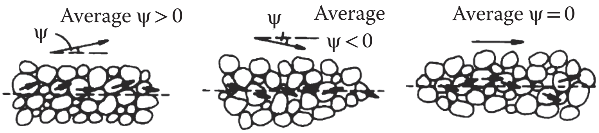

Figure 2.19 Visualisation of rearrangement of soil particles during shear: (a) dilation; (b) contraction; (c) critical state. (Redrawn with permission from Bolton, M.D., *A Guide to Soil Mechanics*, M.D. & K. Bolton, Cambridge, 1991.)

002x019.eps

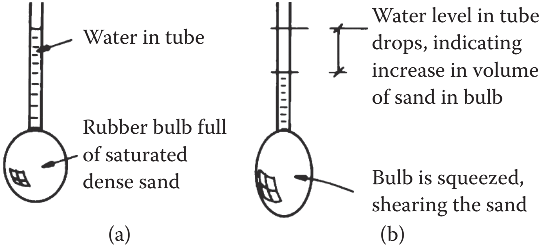

Figure 2.20 Demonstration of dilation: (a) rubber bulb full of saturated dense sand in undisturbed state; (b) what happens when the bulb is squeezed, causing the sand to shear and dilate.

002x020.eps

Courtesy of CRC Press/Taylor & Francis Group

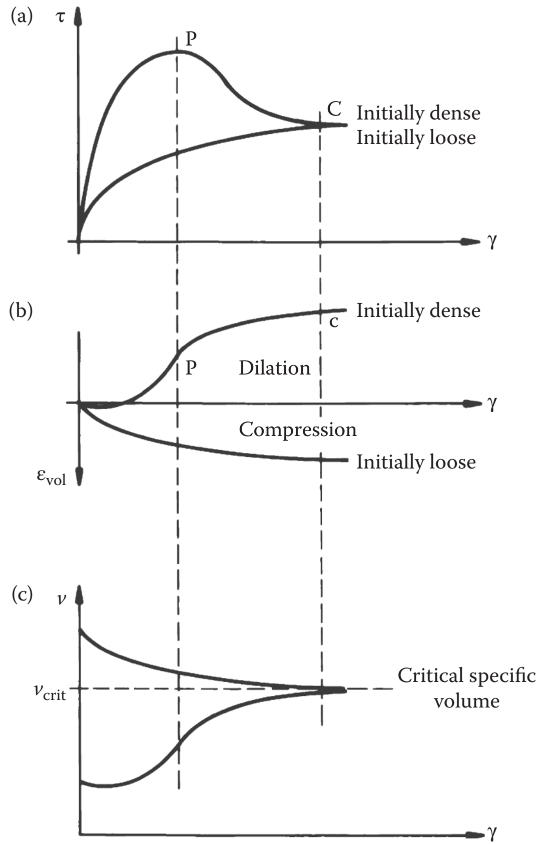

Figure 2.21 Idealised shearbox test results: (a) τ vs γ; (b) ε_{vol} vs γ; (c) v vs γ.

002x021.eps

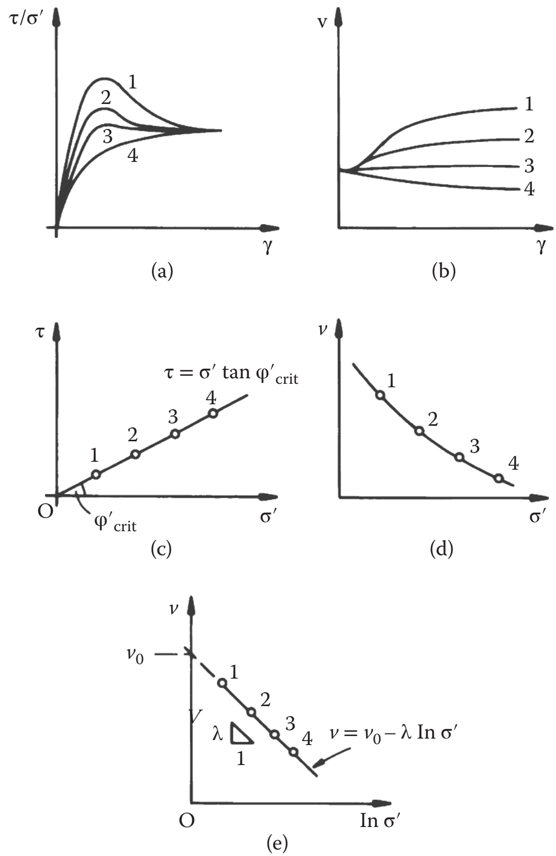

Figure 2.22 Idealised results from shearbox tests, carried out at different normal effective stresses, on four samples having the same initial void ratio: (a) stress ratio τ/σ' vs γ; (b) specific volume ν vs γ; (c) critical states (end points of tests); τ vs σ'; (d) critical states; ν vs σ'; (e) critical states; ν vs $\ln \sigma'$.

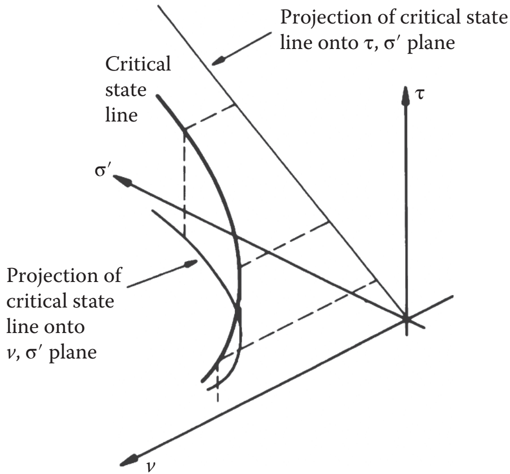

Figure 2.23 Critical state line in (σ', τ, ν) space with projections onto (τ, σ') and (ν, σ') planes.

002x023.eps

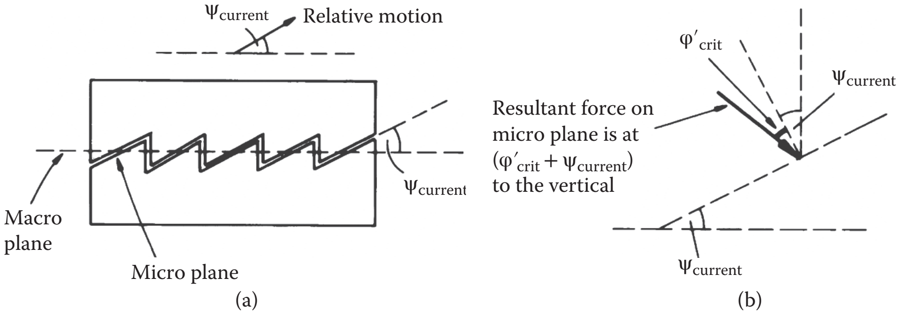

Figure 2.24 (a) $\psi_{current}$ is the current angle of dilation, (b) Sawtooth analogy for dilation. (From Bolton, M.D., *A Guide to Soil Mechanics*, M.D. & K. Bolton, Cambridge, 1991. With permission.)

002x024a.eps 002x024b.eps

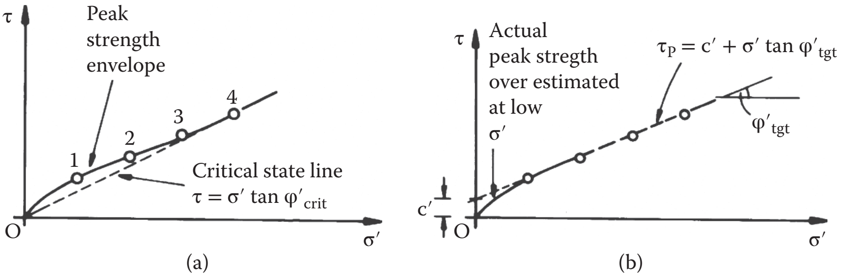

Figure 2.25 (a) Peak strength data, plotted as τ vs σ′, showing curved failure envelope and (b) error associated with simplistic interpretation of peak strength data.

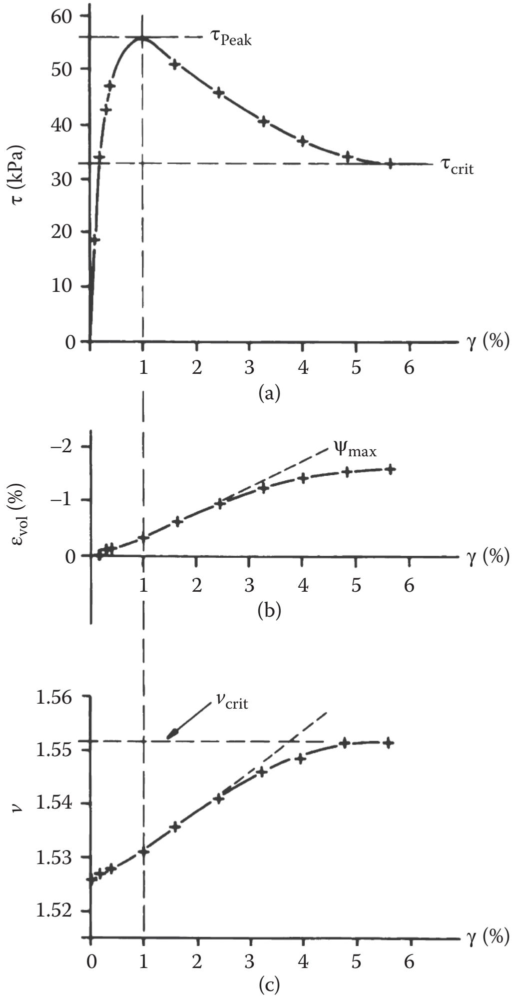

Figure 2.26 Graphs of: (a) shear stress τ against shear strain γ, (b) volumetric strain ε_{vol} against shear strain γ, and (c) specific volume ν against shear strain γ for Example 2.1.

002x026.eps

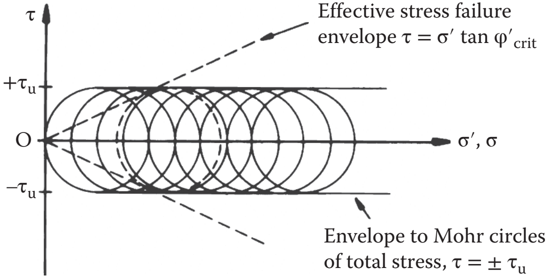

Figure 2.27 Envelope to all possible Mohr circles of total stress at failure for a clay sheared at constant volume.

002x027.eps

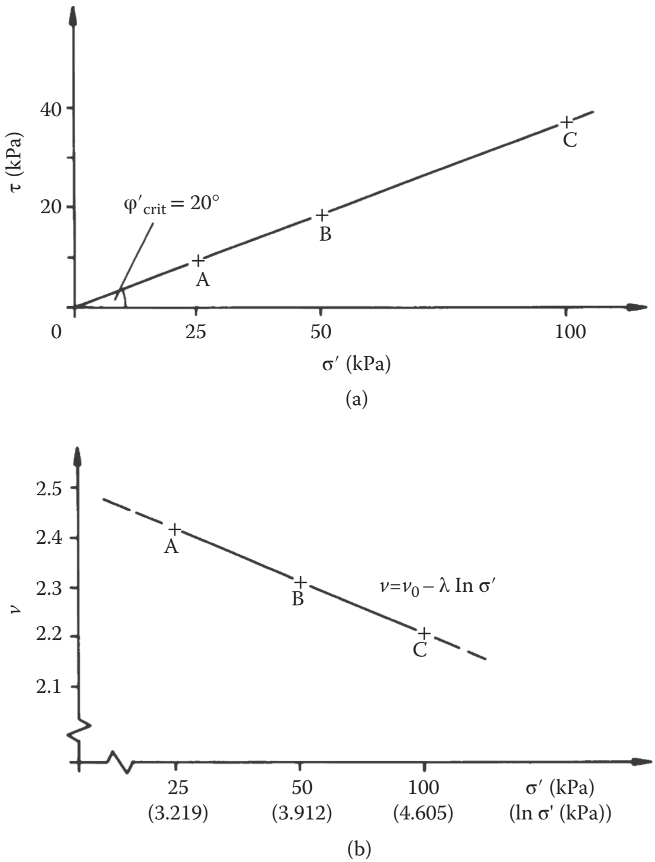

Figure 2.28 (a) τ against σ' and (b) ν against ln σ' for Example 2.2.

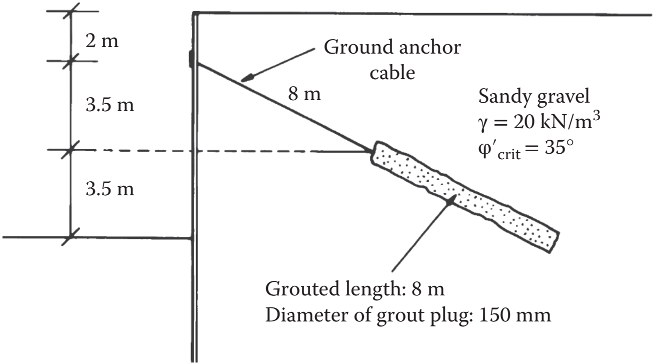

Figure 2.29 Cross-section through grouted ground anchor.

002x029.eps

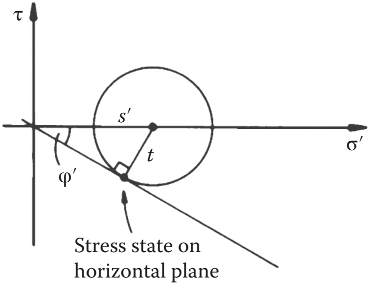

Figure 2.30 Mohr circle of stress for shearbox sample, assuming that the horizontal plane is the plane of maximum stress ratio.

002x030.eps

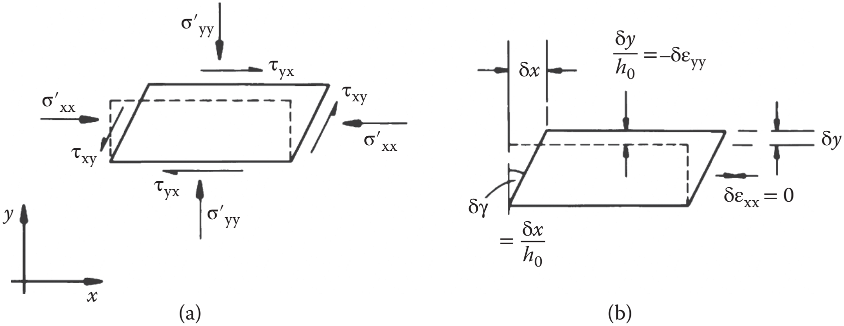

Figure 2.31 For a shearbox test: (a) stresses and (b) plastic strain increments.

002x031.eps

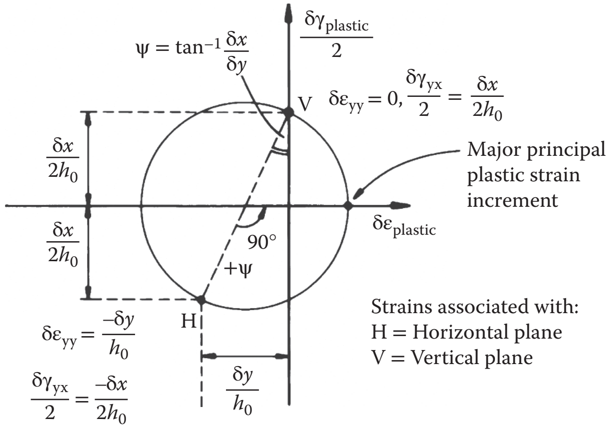

Figure 2.32 Mohr circle of plastic strain increment for a shearbox test.

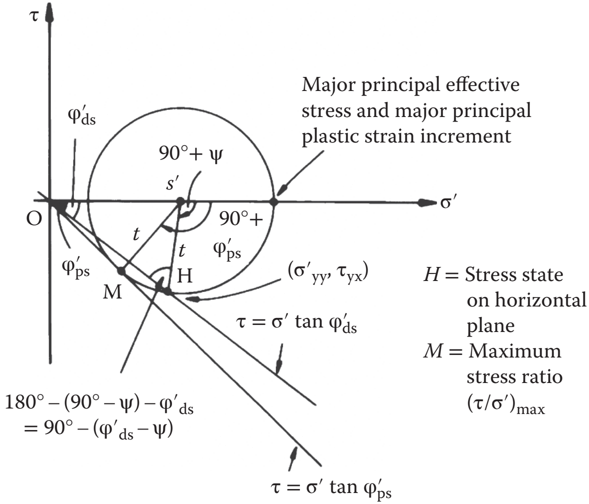

Figure 2.33 Mohr circle of effective stress for shearbox test, assuming that planes of major principal stress and major principal strain increment coincide.

002x033.eps

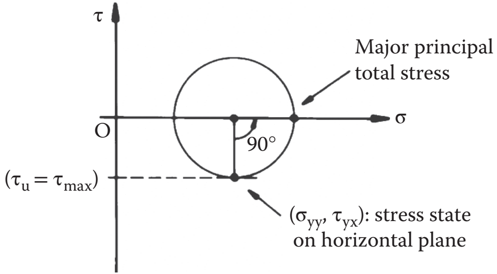

Figure 2.34 Mohr circle of total stress for an undrained shearbox test on a clay, assuming that the horizontal plane is the plane of maximum shear stress.

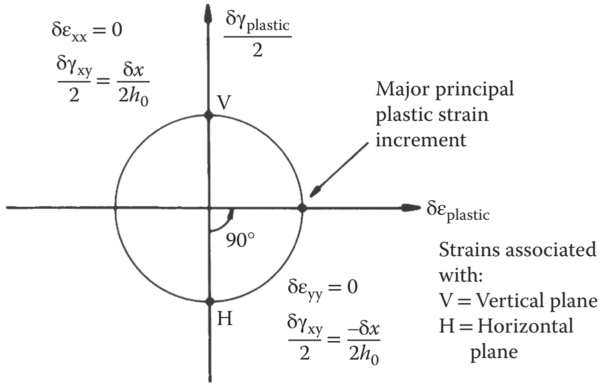

Figure 2.35 Mohr circle of plastic strain increment for an undrained shearbox test on a clay.

002x035.eps

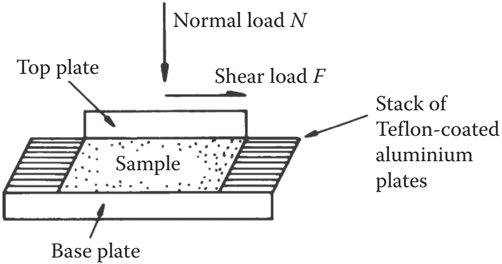

Figure 2.36 Simple shear apparatus. (From Kishida, H. and Uesughi, M., *Géotechnique*, 37, 1, 45–52, 1987. With permission.)

002x036.eps

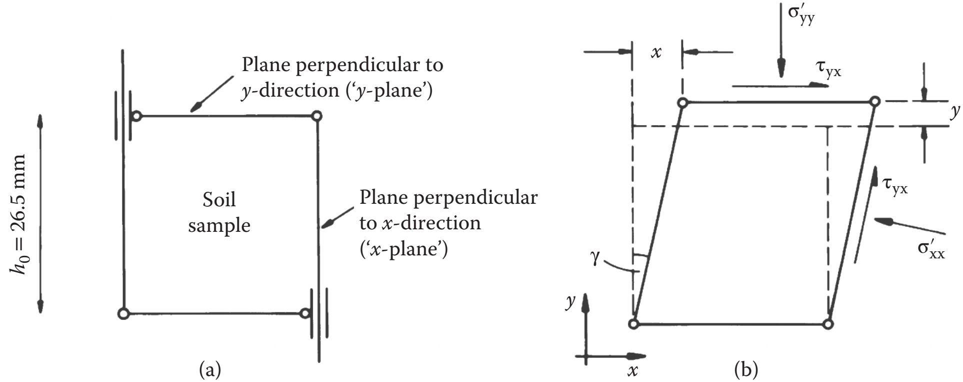

Note: in the direction shown:

τ_{yx} Is clockwise and therefore plots as negative on the Mohr circle of stress

τ_{xy} Is anticlockwise and therefore plots as positive on the Mohr circle of stress

γ_{yx} Involves a clockwise rotation of the material normal with respect to the *y*-plane normal, and therefore plots negative on the Mohr circle of strain (cf. Figure 2.7)

γ_{yx} Involves an anticlockwise rotation of the material normal with respect to the *x*-plane normal, and therefore plots as positive on the Mohr circle of strain

Figure 2.37 Research shearbox: (a) at start of test and (b) during the test.

002x037.eps

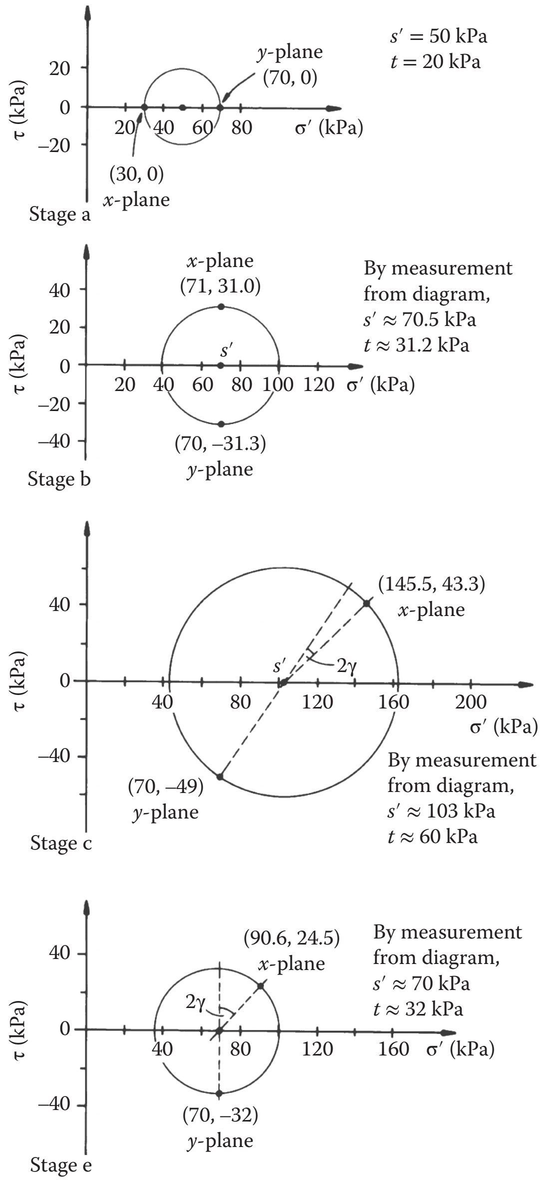

Figure 2.38 Mohr circles of stress for Example 2.5.

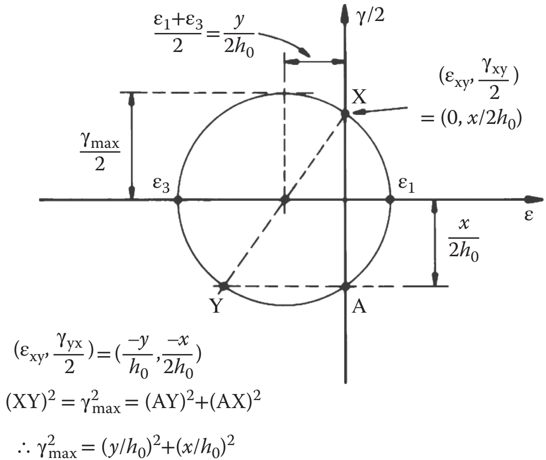

Figure 2.39 Geometry of Mohr circle of strain.

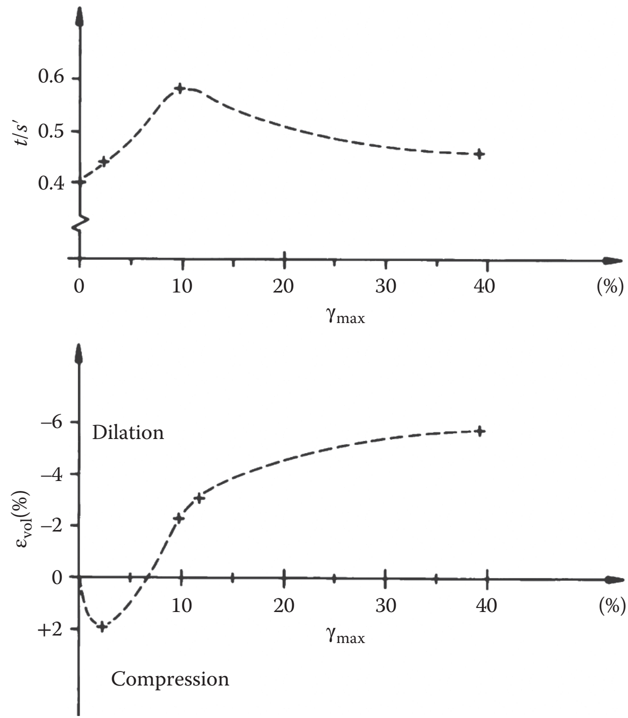

Figure 2.40 Plots of: (a) (t/s') against γ_{max} and (b) ε_{vol} against γ_{max}.